

Temperature-dependent NMR features of the $\text{Al}_{65}\text{Cu}_{20}\text{Ru}_{15}$ icosahedral alloy

E. A. Hill, T. C. Chang,* and Y. Wu†

Department of Physics and Astronomy, University of North Carolina, Chapel Hill, North Carolina 27599

S. J. Poon and F. S. Pierce

Department of Physics, University of Virginia, Charlottesville, Virginia 22901

Z. M. Stadnik

Department of Physics, University of Ottawa, Ottawa, Ontario, Canada K1N 6N5

(Received 25 October 1993)

The $\text{Al}_{65}\text{Cu}_{20}\text{Ru}_{15}$ icosahedral alloy was studied by ^{27}Al nuclear magnetic resonance from 150 to 1110 K. The Knight shift of the unresolved resonance line was observed to significantly increase above 500 K. This uncommon temperature dependence of the Knight shift is interpreted in terms of the presence of a pseudogap at the Fermi level. The spin-lattice relaxation rate deviates from the linear temperature dependence of Korringa relaxation below 500 K, and above 500 K it is dominated by a thermally activated process with a small activation energy of 0.48 eV. This energy is distinctly different from the activation energy observed in simple metallic alloys.

I. INTRODUCTION

The formation of icosahedral (*i*) alloys is an intriguing topic in solid-state physics.^{1,2} One of the central issues is: what mechanism provides the thermal stability observed in some highly ordered *i* alloys such as *i*-Al-Cu-Ru and *i*-Al-Cu-Fe?^{2,3} It is believed that the Fermi surface in *i* alloys falls in the vicinity of some quasi-Brillouin-zone boundaries which interact strongly with the free-electron Fermi surface. As a result, a minimum in the density of states (DOS) appears at the Fermi level, and the structure is stabilized by a significant reduction of the total electronic energy.^{4,5} There is both strong experimental and theoretical evidence for such a pseudogap in *i* alloys.⁶⁻⁸ Other intriguing electronic characteristics, such as the presence of spiky features in the DOS and a minigap (~ 0.05 eV) at the Fermi level which further stabilizes the system, have also been suggested for these alloys.^{6,9} Because nuclear magnetic resonance (NMR) directly probes the DOS and the characteristics of the wave functions around the Fermi level in metals, such novel properties of the DOS might cause uncommon temperature-dependent effects in NMR experiments, in particular at high temperature. Previously, interesting temperature dependences of some NMR parameters have been observed in metals and alloys with novel DOS features at the Fermi level.¹⁰⁻¹² In this work, we report a temperature-dependent Knight shift in *i*-Al-Cu-Ru above 500 K and a deviation from the linear temperature dependence of Korringa relaxation below 500 K.

Another important aspect in the study of *i* alloys is the detection of structural defects and intrinsic dynamic processes.¹³ Phason strains have been detected successfully by diffraction techniques in many *i* alloys.¹⁴ However, such defects are not discernible by diffraction techniques in thermodynamically stable *i* alloys^{2,3} and it is not quite clear whether or not substantial amounts of defects still

remain in some *i* alloys.^{15,16} In addition to previous studies of dynamic phasons,^{13,17} several recent investigations have addressed the issue of novel dynamic processes in *i* alloys. For instance, a new self-diffusion process (one other than monovacancy-assisted atomic diffusion) has been proposed for quasiperiodic structures,¹⁸ while collective motions and localized vibrations (involving atomic clusters of about 10-Å size) have been the focus of current experiments.^{19,20} With these efforts in mind, there is considerable interest in further experimental information on dynamic processes in *i* alloys. In the past, the spin-lattice relaxation of quadrupolar nuclei has been used extensively to study diffusion processes²¹ and structural defects, including atomic tunneling states in amorphous materials.²² Atomic motions contribute effectively to the spin-lattice relaxation of quadrupolar nuclei by modulating the local electric field gradient (EFG).^{23,24} Thus, ^{27}Al NMR in some *i* alloys may prove to be very useful for detecting intrinsic dynamic processes, as well as motions associated with structural defects. In this work, we report an extremely effective spin-lattice relaxation process in *i*-Al-Cu-Ru detected by ^{27}Al NMR measurements at high temperature. This relaxation process has an apparent activation energy that is significantly smaller than that of monovacancy-assisted diffusion observed in conventional metals.

II. EXPERIMENTAL

Ribbons of *i*- $\text{Al}_{65}\text{Cu}_{20}\text{Ru}_{15}$ were fabricated by melt spinning and were subsequently annealed at 1073 K for 24 hours.²⁵ The NMR experiments were carried out on a Chemagnetics CMX400 spectrometer at 9.4 T with a home-built high-temperature probe. The ^{27}Al resonance frequency is at 104.23 MHz. Because the ^{27}Al satellite transitions are broadened by the first-order quadrupolar effect,^{23,24} only the ^{27}Al $\frac{1}{2} \leftrightarrow -\frac{1}{2}$ central transition (about

60 kHz wide in this sample) was observed with a Hahn echo pulse technique. Nuclear spin-lattice relaxation rates were measured by an inversion-recovery method incorporating a $90^\circ_x-240^\circ_y-90^\circ_x$ composite inversion pulse²⁶ and Hahn echo detection. Hard pulses ($\pi/2$ pulses were between 2 and 4 μs) and a low- Q rf circuit were used, allowing uniform irradiation of the entire central transition but minimal excitation of the satellite transitions in the spin-lattice relaxation experiments. All of the experimental results can be repeated after several heating cycles.

III. RESULTS AND DISCUSSION

Figures 1(a), (b), and (c) show the ^{27}Al spectra of $i\text{-Al}_{65}\text{Cu}_{20}\text{Ru}_{15}$ at room temperature, 873, and 1110 K, respectively. No change of the spectrum can be noticed up to 500 K. The shift at room temperature is at about 150 ppm [with respect to the shift of ^{27}Al in aqueous $\text{Al}(\text{NO}_3)_3$ solution], as has been observed before.²⁷⁻³² For comparison, Fig. 1(d) shows the ^{27}Al spectrum at 973 K of the crystal (c) $\text{Al}_7\text{Cu}_2\text{Fe}$, a good metal with a resistivity of 16 $\mu\Omega\text{ cm}$ at 4.2 K (compared to $> 10000\mu\Omega\text{ cm}$ in $i\text{-Al}_{65}\text{Cu}_{20}\text{Ru}_{15}$); the shift of the peak is at 450 ppm and is temperature independent. In contrast, the shift in $i\text{-Al}_{65}\text{Cu}_{20}\text{Ru}_{15}$ changes significantly above the Debye temperature (500 K), as shown in Fig. 2. The peak at 1110 K, for instance, is shifted to 420 ppm.

Figures 3(a) and (b) display magnetization recovery data at a selection of temperatures for ^{27}Al in $i\text{-Al}_{65}\text{Cu}_{20}\text{Ru}_{15}$ and $c\text{-Al}_7\text{Cu}_2\text{Fe}$, respectively. For reasons discussed below, the quantity M^* , defined by

$$M^* \equiv \frac{M_\infty - M(\tau)}{M_\infty - M_0}, \quad (1)$$

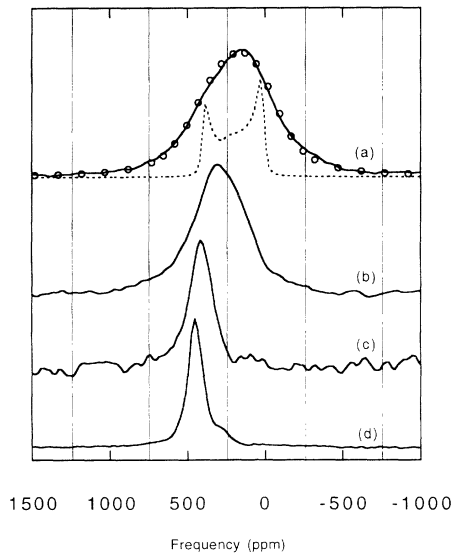


FIG. 1. ^{27}Al spectra of $i\text{-Al}_{65}\text{Cu}_{20}\text{Ru}_{15}$ at (a) room temperature, (b) 873 K, and (c) 1110 K. (d) ^{27}Al spectrum of crystalline $\text{Al}_7\text{Cu}_2\text{Fe}$ at 973 K. The circles indicate a numerical powder-pattern simulation of the room-temperature spectrum with linewidth broadening. The dashed line is the same simulation with only nominal broadening.

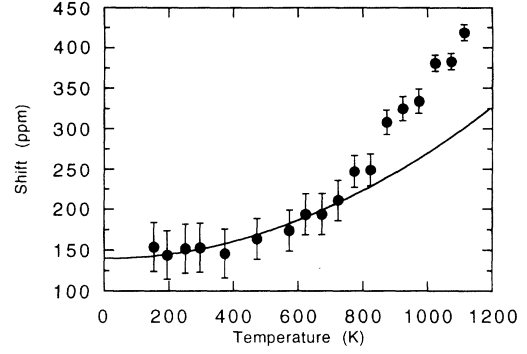


FIG. 2. Measured ^{27}Al shift vs the temperature for $i\text{-Al}_{65}\text{Cu}_{20}\text{Ru}_{15}$. The shift increases from 150 ppm at room temperature to 420 ppm at 1110 K. The solid line is a fit based on Eq. (4) of the text; the constant coefficient is 130 ppm and the T^2 coefficient is $1.3 \times 10^{-4} \text{ ppm/K}^2$.

is plotted versus τT , where M_∞ is the magnetization at equilibrium, M_0 is the initial magnetization after inversion, $M(\tau)$ is the magnetization at the recovery time τ , and T is the absolute temperature. Figure 4 shows the temperature dependence of the magnetization recovery rate R for ^{27}Al in $i\text{-Al}_{65}\text{Cu}_{20}\text{Ru}_{15}$ and $c\text{-Al}_7\text{Cu}_2\text{Fe}$. R is defined as the inverse of the time interval during which M^* decays by a factor of $1/e$.

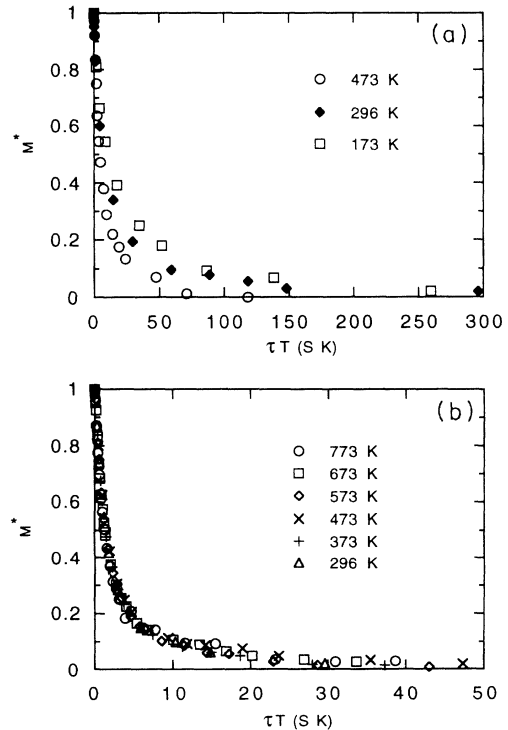


FIG. 3. Function M^* (see text) versus the product of the magnetization recovery time and the absolute temperature (τT) for (a) $i\text{-Al}_{65}\text{Cu}_{20}\text{Ru}_{15}$ and (b) crystalline $\text{Al}_7\text{Cu}_2\text{Fe}$ at various temperatures.

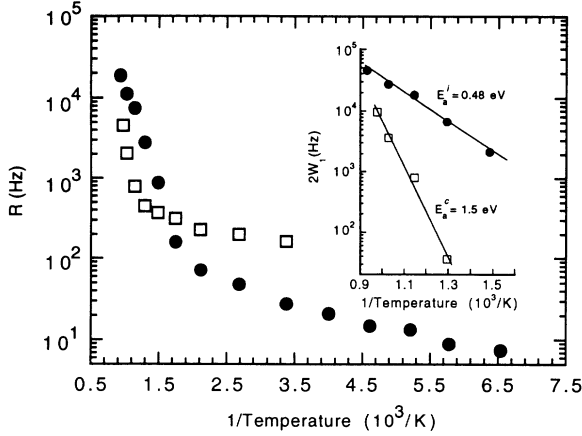


FIG. 4. Magnetization recovery rate R versus the inverse of the temperature for $i\text{-Al}_{65}\text{Cu}_{20}\text{Ru}_{15}$ (●) and crystalline $\text{Al}_7\text{Cu}_2\text{Fe}$ (□). The inset displays the spin-lattice relaxation rate $2W_1$ ($=1/T_1$) versus the inverse of the temperature in the high-temperature regime. The Korringa relaxation has been subtracted from $2W_1$ for $\text{Al}_7\text{Cu}_2\text{Fe}$.

A. The Knight shift

The ^{27}Al resonance line in $i\text{-Al}_{65}\text{Cu}_{20}\text{Ru}_{15}$ is broadened by the isotropic second-order quadrupolar interaction, Knight shift anisotropy, and a distribution of local environments. The ^{27}Al resonance shift in $i\text{-Al}_{65}\text{Cu}_{20}\text{Ru}_{15}$ consists of the sum of the chemical shift, the second-order isotropic quadrupolar shift, and the Knight shift. The ^{27}Al chemical shift typically ranges from 0 to about 200 ppm.³³ The second-order isotropic quadrupolar shift is given by²³

$$\delta_{\text{iso}}^{(2)} = -\frac{1}{30} \frac{\nu_Q^2}{\nu_L} \left[1 + \frac{\eta^2}{3} \right] \left[I(I+1) - \frac{3}{4} \right], \quad (2)$$

where $\nu_Q = 3e^2qQ/2I(2I-1)h$ is the quadrupole frequency, ν_L is the Larmor frequency, and η is the asymmetry parameter of the EFG tensor. The upper limit of the quadrupole frequency ν_Q can be estimated by a line-shape simulation which assumes that the observed linewidth arises mainly from the anisotropic second-order quadrupolar interaction. The resulting orientation dependence of the resonance frequency is given by^{23,34}

$$\nu_{\text{aniso}}^{(2)} = \sum_{l=0,2,4} \sum_{\substack{|m| \leq l \\ \text{even}}} \alpha_{lm} Y_{lm}(\theta, \varphi), \quad (3)$$

where α_{lm} depends on the Larmor frequency ν_L , the quadrupole frequency ν_Q , and the asymmetry parameter η ; Y_{lm} are spherical harmonics and θ and φ are the polar coordinates of the magnetic field with respect to the principal-axes systems of the EFG tensor. The powder-pattern simulation based on the anisotropic second-order quadrupolar interaction³⁴ is shown in Fig.1 for the room-temperature spectrum with $\nu_Q = 1.7$ MHz, $\eta = 0$, and a linewidth broadening to smooth out prominent features of the powder pattern which are clearly absent in the observed spectrum. This puts a limit for the largest

negative shift $\delta_{\text{iso}}^{(2)}$ at -70 ppm. An analogous powder-pattern simulation of the spectrum at 1110 K, which yields a value of $\delta_{\text{iso}}^{(2)} = -30$ ppm, indicates that the quadrupolar interaction contributes a shift change of about 40 ppm or less in these experiments.

The Knight shift is typically the dominant resonance shift in metals and metallic alloys^{35,56} and is usually temperature independent. For instance, the 450-ppm shift observed in $c\text{-Al}_7\text{Cu}_2\text{Fe}$ can be attributed almost completely to the Knight shift, as confirmed by the spin-lattice relaxation measurements discussed below. The large shift increase to 430 ppm observed in $i\text{-Al}_{65}\text{Cu}_{20}\text{Ru}_{15}$ at high temperature is too large to be accounted for by the chemical shift or the change of $\delta_{\text{iso}}^{(2)}$. Therefore, the observed shift change of more than 250 ppm has to be attributed to an increase of the Knight shift. Although the Knight shift is essentially temperature independent in most materials, there are some specific cases where it does change significantly with temperature.^{10,12} One mechanism for such changes arises from the presence of sharp features in the DOS around the Fermi level. Assuming that the DOS function is temperature independent, the temperature dependence from the Knight shift can be expressed as³⁶

$$K(T) = K^0 \left\{ 1 + \frac{\pi^2 k_B^2}{6} \left[\frac{g''(E_F^0)}{g(E_F^0)} - \left(\frac{g'(E_F^0)}{g(E_F^0)} \right)^2 \right] T^2 \right\}, \quad (4)$$

where $g(E)$ is the DOS for a single spin orientation, $g'(E)$ is its first derivative, $g''(E)$ is its second derivative, E_F^0 is the Fermi energy at 0 K, K^0 is the low-temperature limit of the Knight shift, and k_B is the Boltzmann constant. K^0 can be expressed as³⁵

$$K^0 = \frac{4}{3} \pi \hbar^2 \gamma_e^2 \langle |u_k^2(0)| \rangle_{E_F^0} g(E_F^0), \quad (5)$$

where $\langle |u_k^2(0)| \rangle_{E_F^0}$ is the density of the wave function at the nucleus averaged over the Fermi surface and γ_e is the gyromagnetic ratio of the electron. No temperature dependence of K can be observed in most metals and alloys because $g'(E_F^0)$ and $g''(E_F^0)$ are quite small while $g(E_F^0)$ is quite large. However, as mentioned above, sharp features in the DOS and the presence of a pseudogap have been predicted for i alloys and their approximant phases. Therefore, this mechanism might contribute to the observed temperature dependence of the ^{27}Al Knight shift in $i\text{-Al}_{65}\text{Cu}_{20}\text{Ru}_{15}$. A fit based on the functional form of Eq. (4) is shown in Fig. 2. It is difficult to account for the observed temperature dependence of the Knight shift over the entire temperature range based on this mechanism. In fact, the assumption of a temperature-independent band structure used in the previous discussion may no longer be valid above the Debye temperature. The creation of a pseudogap or sharp features of the DOS depends on a strong effect of the pseudopotential.⁵ Since the pseudopotential is proportional to the effective structure factor $S_{\bar{G}}(T) = \exp[-W_{\bar{G}}(T)]S_{\bar{G}}(0)$, it decreases as the temperature increases because of the reduction of the Debye-

Waller factor $\{\exp[-2W_{\bar{c}}(T)]\}$. As a result, the system may become more free-electron-like at high temperatures. The DOS at the Fermi level will increase and the characteristics of the wave functions at the Fermi level will also change. Consequently, the Knight shift might also vary with temperature (note the similarity of the $i\text{-Al}_{65}\text{Cu}_{20}\text{Ru}_{15}$ and $c\text{-Al}_7\text{Cu}_2\text{Fe}$ shifts at high temperature). This effect has been demonstrated to be responsible for the increase of the Knight shift at high temperature in Cd metal.^{10,11} This interpretation of the Knight shift data indicates a significant change of the electronic DOS and the characteristics of the wave functions above the Debye temperature.

B. The spin-lattice relaxation

For convenience of discussion, the nuclear spin-lattice relaxation data are considered to have two temperature regimes, below and above 500 K. Typically, the nuclear spin-lattice relaxation in metallic alloys is dominated at low temperature by Korringa relaxation.^{35,36} The inversion-recovery of the central transition for spin- $\frac{5}{2}$ nuclei under the Korringa relaxation mechanism is governed by^{37,38}

$$M(\tau) = M_{\infty} [1 - 0.057 \exp(-2W_1\tau) - 0.356 \exp(-12W_1\tau) - 1.587 \exp(-30W_1\tau)], \quad (6)$$

where $2W_1$ is the spin-lattice relaxation rate. Figure 5 shows $2W_1$ values, which are obtained by a least-squares fit of the inversion-recovery curves with Eq. (6), for $i\text{-Al}_{65}\text{Cu}_{20}\text{Ru}_{15}$ at temperatures below 500 K. The fits of the magnetization recovery are reasonably good, although not perfect. Partial excitation of the ^{27}Al satellite transitions and cross relaxation to the ^{63}Cu satellite transitions could be responsible for the small discrepancy. Figure 5 shows that the temperature dependence of $2W_1$ deviates from the expected linear dependence of the Korringa relaxation commonly observed in metals and alloys.

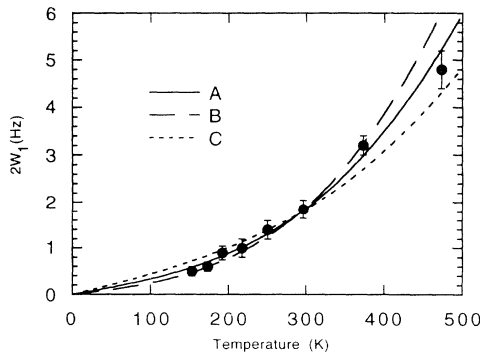


FIG. 5. Spin-lattice relaxation rate $2W_1$ versus the temperature for $i\text{-Al}_{65}\text{Cu}_{20}\text{Ru}_{15}$ in the low-temperature regime. The theoretical fits A, B, and C have coefficients of 3×10^{-3} , 2×10^{-3} , and 4.2×10^{-3} Hz/K for the linear term and coefficients of 3.6×10^{-8} , 4.8×10^{-8} , and 2.2×10^{-8} Hz/K³ for the cubic term, respectively.

Evidence of this deviation also appears in Fig. 3(a); the M^* -versus- τT curves of $i\text{-Al}_{65}\text{Cu}_{20}\text{Ru}_{15}$ at different temperatures do not overlay one another. A linear temperature dependence of the relaxation rate causes these curves to overlay, as seen for $c\text{-Al}_7\text{Cu}_2\text{Fe}$ in Fig. 3(b). Nonlinear temperature dependence of the spin-lattice relaxation may result from the higher-order effect of Korringa relaxation. The expression for Korringa relaxation carried out to higher-order terms is given by³⁹

$$\frac{1}{T_1} \equiv 2W_1 = \frac{64}{9} \pi^3 \hbar^3 k_B \gamma_e^2 \gamma_n^2 \langle |u_k^2(0)| \rangle_{E_F^0}^2 g(E_F^0)^2 \times \left[T + \frac{\pi^2 k_B^2}{3} \frac{g''(E_F^0)}{g(E_F^0)} T^3 \right], \quad (7)$$

where T_1 is the nuclear spin-lattice relaxation time and γ_n is the gyromagnetic ratio of the observed nucleus. Considering the presence of the pseudogap which leads to a small $g(E_F^0)$ and possibly a large $g''(E_F^0)$, the nonlinear temperature dependence of $1/T_1$ could be anticipated. Using expression (7), a fit (A) with $g''(E_F^0)/g(E_F^0) = 500 \text{ eV}^{-2}$ is shown in Fig. 5. Fits with $g''(E_F^0)/g(E_F^0) = 1000 \text{ eV}^{-2}$ (B) and $g''(E_F^0)/g(E_F^0) = 250 \text{ eV}^{-2}$ (C) are shown to indicate the accuracy of (A). The products of $T_1^i T = T/2W_1$ (i refers to $i\text{-Al}_{65}\text{Cu}_{20}\text{Ru}_{15}$) in the low-temperature limit, as determined from the linear part of these fittings, are 333 (A), 500 (B), and 238 s K (C), respectively. For pure Al, $T_1^{\text{Al}} T = 1.85 \text{ s K}$ (the superscript (subscript) Al refers to Al metal) and $K_{\text{Al}}^0 = 1600 \text{ ppm}$. The low-temperature Knight shift of $i\text{-Al}_{65}\text{Cu}_{20}\text{Ru}_{15}$, K_i^0 , can be estimated by $T_1^i T (K_i^0)^2 = T_1^{\text{Al}} T (K_{\text{Al}}^0)^2$, which gives $K_i^0 = 120 \text{ ppm}$ with $T_1^i T = 333 \text{ s K}$. This is close to the measured low-temperature shift of 150 ppm. This shows that the estimation of the low-temperature Knight shift based on the Korringa relaxation mechanism agrees in order of magnitude with the measured shift value. Note that the nuclear spin-lattice relaxation in $c\text{-Al}_7\text{Cu}_2\text{Fe}$ has the conventional linear temperature dependence for $2W_1$ up to 600 K with $T_1^c T = 28 \pm 2 \text{ s K}$ (c refers to $c\text{-Al}_7\text{Cu}_2\text{Fe}$). The predicted Knight shift for $c\text{-Al}_7\text{Cu}_2\text{Fe}$, using $T_1^c T (K_c^0)^2 = T_1^{\text{Al}} T (K_{\text{Al}}^0)^2$, is 411 ppm [compared to the measured shift of 450 ppm, see Fig. 1(d)]. Another parameter ξ^i , defined by $\xi^i = \langle |u_k^2(0)| \rangle_{E_F^0} / \langle |u_k^2(0)|_{\text{Al}} \rangle_{E_F^0}^{-1}$, describes the characteristics of the wave function at the Fermi level. Since Al metal can be almost perfectly accounted for by the nearly-free-electron (NFE) model, deviation of ξ^i from 1 provides a measure of the departure from the NFE wave function. Using the linear part of $1/T_1$, ξ^i can be expressed as $\xi^i = g^{\text{Al}}(E_F^0) \sqrt{T_1^{\text{Al}} T} [g^i(E_F^0) \sqrt{T_1^i T}]^{-1}$.³⁵ The experimental value of $g^i(E_F^0)$ as determined by specific-heat measurement²⁵ on this sample is $3.8 \times 10^{21} \text{ cm}^{-3} \text{ eV}^{-1}$; the value of $g^{\text{Al}}(E_F^0)$ is $3.2 \times 10^{22} \text{ cm}^{-3} \text{ eV}^{-1}$. The relaxation data and these DOS values give $\xi^i = 0.62$ for $T_1^i T = 333 \text{ s K}$. This indicates less s character in the wave function compared to the NFE model. It should be emphasized that, although the derived value of $g''(E_F^0)$ can be used to evaluate the DOS features, such an evaluation cannot be reliably extended beyond a few $k_B T$ from

the Fermi level.

There is some uncertainty associated with the above explanation based on the higher-order Korringa relaxation effect. Since the ^{27}Al shift is constant below 500 K, Eq. (4) implies that the value of $g''(E_F^0)/g(E_F^0)$ has to be compensated by the value of the square of $g'(E_F^0)/g(E_F^0)$ below 500 K. Although this is possible [the contributions from $g''(E_F^0)$ and $g'(E_F^0)$ have opposite signs in this case] and the resolution of the spectra at low temperatures does not allow the observation of small shift changes, this requirement of compensation should at least be considered as a factor of uncertainty in the explanation. Thus, other explanations should also be considered for the nonlinear temperature dependence of the nuclear spin-lattice relaxation in $i\text{-Al}_{65}\text{Cu}_{20}\text{Ru}_{15}$ below 500 K. It is well known that dynamic processes such as phonons and atomic tunneling states can contribute to the spin-lattice relaxation of quadrupolar nuclei in this temperature regime. Although the nuclear spin-lattice relaxation times associated with phonons are much longer than those observed here for $i\text{-Al}_{65}\text{Cu}_{20}\text{Ru}_{15}$,⁴⁰ tunneling states have been shown to cause effective spin-lattice relaxation for quadrupolar nuclei in vitreous glasses.²² Moreover, there is experimental evidence for intrinsic (i.e., nondefective) atomic tunneling states in a high quality Al-Pd-Mn i alloy.¹⁵ Thus, a quadrupolar relaxation mechanism due to a dynamic process is not unreasonable in the present case of a noncrystalline sample with a low DOS at the Fermi level. Further investigation, such as introducing defects into the sample, is required to test the presence of such a relaxation mechanism.

The dramatic increase of the ^{27}Al nuclear spin-lattice relaxation rate above 500 K in both samples is attributed to quadrupolar relaxation caused by the thermally activated motion of atoms. Both single- and double-quantum transitions (with rates W_1 and W_2) between the spin energy levels can be induced by the EFG fluctuations due to such motion. The standard assumption that an exponential correlation function describes these fluctuations leads to the relations $W_1 = \alpha\tau_c [1 + (\omega_0\tau_c)^2]^{-1}$ and $W_2 = \alpha\tau_c [1 + (2\omega_0\tau_c)^2]^{-1}$, where α is a constant, τ_c is the correlation time of the motion, and ω_0 is the angular Larmor frequency.^{23,24} Given that τ_c is of the form $\tau_c(T) = \tau_c(\infty) \exp(-E_a/k_B T)$, the activation energy E_a can be extracted from the temperature dependence of $2W_1$ in the low-temperature or high-temperature limits, where τ_c and ω_0 satisfy the conditions $(\omega_0\tau_c)^2 \gg 1$ or $(\omega_0\tau_c)^2 \ll 1$, respectively. The rate $2W_1$, shown in the inset of Fig. 4, is determined by using³⁷

$$M(\tau) = M_\infty [1 - 0.003 \exp(-2.41 W_1 \tau) - 0.3 \exp(-0.26 W_1 \tau) - 1.697 \exp(-0.83 W_1 \tau)], \quad (8)$$

which assumes $W_2 \approx W_1/4$, a consequence of the low-temperature limit in the present case. The temperature dependence of W_1 for $i\text{-Al}_{65}\text{Cu}_{20}\text{Ru}_{15}$ can be fit by $W_1(T) = W_1(\infty) \exp(-E_a/k_B T)$ with $E_a^i = 0.48 \pm 0.03$ eV and $W_1^i(\infty) = 4.2 \times 10^6$ Hz (see Fig. 4 inset). This result was reproducible after several heating cycles. The atomic

self-diffusion process in Al metal and alloys has been studied extensively by NMR.¹² Commonly observed activation energies are about 1.3–1.5 eV (attributed to the formation and migration of monovacancies) in agreement with the 1.50 ± 0.05 eV measured in $c\text{-Al}_7\text{Cu}_2\text{Fe}$ (see Fig. 4 inset).

Clearly, the process dominating the spin-lattice relaxation in $i\text{-Al}_{65}\text{Cu}_{20}\text{Ru}_{15}$ above 500 K is quite different from monovacancy-assisted atomic diffusion. Motions of residual defects with a low energy barrier may cause such efficient relaxation, but it is not clear how these defects could survive the annealing during sample preparation and several heating cycles during high-temperature measurements. The spin-lattice relaxation observed in $i\text{-Al}_{62}\text{Cu}_{25.5}\text{Fe}_{12.5}$ may be caused by intrinsic atomic motions which could be different from those found in simple metals and alloys. As mentioned earlier, localized vibrations of atomic clusters (about 10 Å in length scale) which are excited at high temperature have been reported in $i\text{-Al}_{65}\text{Cu}_{20}\text{Fe}_{15}$ recently.²⁰ Such localized vibrational modes may cause efficient spin-lattice relaxation by modulating the EFG. The activation process determined from the present experiment does not necessarily imply that the corresponding dynamic process has a unique activation energy of 0.48 eV. Collective motions involving more than one atom often lead to a nonexponential correlation function.⁴¹ The collective aspect of the motion manifests itself mainly in the short-time behavior of the correlation function, and the high-frequency range of the Fourier spectrum of the correlation function corresponds to the short-time behavior of the correlation function.⁴¹ Thus, the spin-lattice relaxation measurement in the low-temperature limit (where the Larmor frequency is at the high-frequency range of the Fourier spectrum of the correlation function) probes mainly the collective aspect of the dynamic process. Since collective motions encounter lower energy barriers than single-atom motions, the apparent activation energy determined in the low-temperature limit can be smaller than the one determined in the high-temperature limit. The high-temperature limit in the current experiment, however, requires measurements at temperatures higher than the melting temperature of the material. Further investigation is necessary to determine the exact nature of this dynamic process; nevertheless, its presence in $i\text{-Al}_{65}\text{Cu}_{20}\text{Ru}_{15}$ is very obvious. The spin-lattice relaxation rate of ^{27}Al in $i\text{-Al}_{65}\text{Cu}_{20}\text{Ru}_{15}$ changes by over two orders of magnitude between 723 and 1073 K. The quadrupolar relaxation in $i\text{-Al}_{65}\text{Cu}_{20}\text{Ru}_{15}$ is over two orders of magnitude faster than it is in $c\text{-Al}_7\text{Cu}_2\text{Fe}$ at 773 K. These facts indicate that the influence of the high-temperature atomic motion on the spin-lattice relaxation in $i\text{-Al}_{65}\text{Cu}_{20}\text{Ru}_{15}$ is quite unlike the case of a simple crystalline alloy.⁴²

IV. CONCLUSION

In summary, the unusual temperature dependence of the ^{27}Al Knight shift in $i\text{-Al}_{65}\text{Cu}_{20}\text{Ru}_{15}$ has been examined in the context of two different mechanisms. One of these mechanisms is the result of sharp structure in the electronic density of states near the Fermi level, which

influences the Knight shift via the electronic statistics. The other mechanism relies on temperature-dependent changes in the electronic density of states and electronic wave functions at the Fermi level due to atomic vibrations above the Debye temperature. The nonlinear temperature dependence of the nuclear spin-lattice relaxation below the Debye temperature has been described in terms of an electronic relaxation mechanism, but quadrupolar relaxation due to atomic motion cannot be ruled out. The nuclear spin-lattice relaxation above the Debye temperature reveals the existence of a thermally activated process with an apparent activation energy of 0.48 eV. It has been found that this spin-lattice relaxation mecha-

nism is markedly different from the relaxation mechanism associated with monovacancy-assisted self-diffusion found in conventional simple metallic alloys.

ACKNOWLEDGMENTS

The authors thank Dr. H. Kessemeier, Dr. J. P. Lu, Dr. K. Dy, L. Slifkin, Dr. J. E. S. Socolar, and Dr. J. C. Austin for useful conversations. This work was supported by the National Science Foundation under contracts DMR-9122992 and DMR-9015538, and by the National Science and Engineering Research Council of Canada.

*Present address: Industrial Technology Research Institute, Hsinchu, Taiwan 300, People's Republic of China.

[†]Author to whom correspondence should be addressed.

¹D. Shechtman *et al.*, Phys. Rev. Lett. **53**, 1951 (1984).

²For the most recent reviews, see, for example, papers in *Quasicrystals: The State of the Art*, Vol. 11 of *Directions in Condensed Matter Physics*, edited by D. P. Divincenzo and P. J. Steinhardt (World Scientific, Singapore, 1991).

³A. P. Tasi, in *Physics and Chemistry of Finite Systems: From Clusters to Crystals*, Vol. II of *Advanced Study Institute, Series B: Physics*, edited by P. Jena *et al.* (Kluwer, Boston, 1992), p. 39; C. A. Guryan *et al.*, Phys. Rev. Lett. **62**, 2409 (1989).

⁴P. A. Bancel and P. A. Heiney, Phys. Rev. B **33**, 7917 (1986); J. Friedel, Helv. Phys. Acta **61**, 538 (1988); V. G. Vaks *et al.*, Phys. Lett. A **132**, 131 (1988); J. L. Wagner *et al.*, Phys. Rev. Lett. **65**, 203 (1990).

⁵A. P. Smith and N. W. Ashcroft, Phys. Rev. Lett. **59**, 1365 (1987).

⁶F. Fujiwara and H. Tsunetsugu, in *Quasicrystals: The State of the Art* (Ref. 2), p. 343; T. Fujiwara, Phys. Rev. B **40**, 942 (1989).

⁷J. Hafner and M. Krajač, Phys. Rev. Lett. **68**, 2321 (1992); Europhys. Lett. **17**, 145 (1992).

⁸A. Sadoc *et al.* J. Non-Cryst. Solids **153&154**, 338 (1993).

⁹J. C. Phillips, Phys. Rev. B **47**, 2522 (1993).

¹⁰E. F. W. Seymour and G. A. Styles, Phys. Lett. **10**, 269 (1964).

¹¹R. V. Kasowski and L. M. Falicov, Phys. Rev. Lett. **22**, 1001 (1969).

¹²V. Jaccarino *et al.*, Phys. Rev. Lett. **21**, 1811 (1968); A. C. Switendick and A. Narath, *ibid.* **22**, 1423 (1969); G. C. Carter *et al.*, Phys. Rev. B **5**, 3621 (1972).

¹³T. C. Lubensky, in *Introduction to Quasicrystals*, edited by M. Jaric (Academic, Boston, 1988).

¹⁴See, for example, P. A. Heiney *et al.*, Science **238**, 660 (1987).

¹⁵N. Vernier *et al.*, Europhys. Lett. **22**, 187 (1993).

¹⁶N. O. Birge *et al.*, Phys. Rev. B **36**, 7685 (1987).

¹⁷P. A. Bancel, Phys. Rev. Lett. **63**, 2741 (1989).

¹⁸P. A. Kalugin and A. Katz, Europhys. Lett. **29**, 921 (1993).

¹⁹G. Coddens *et al.*, Europhys. Lett. **16**, 271 (1991).

²⁰C. Janot *et al.*, Phys. Rev. Lett. **71**, 871 (1993).

²¹A. Seeger *et al.*, Phys. Status Solidi B **48**, 481 (1971); S. Dais *et al.*, in *Vacancies and Interstitials in Metals and Alloys*,

Vols. 15–18, Part 1 of *Materials Science Forum*, edited by C. Abromeit and H. Wollenberger (Trans. Tech., Aedermannsdorf, 1987), p. 419; Y. Chabre, J. Phys. F **4**, 626 (1974); L. Bottyan *et al.*, Phys. Status Solidi B **118**, 835 (1983).

²²See, for example, M. Rubinstein and H. A. Resing, Phys. Rev. B **13**, 959 (1976); J. Szeftel and H. Alloul, J. Non-Cryst. Solids **29**, 253 (1978).

²³M. H. Cohen and F. Reif, in *Solid State Advances in Research and Applications*, edited by F. Seitz and D. Turnbull (Academic, New York, 1957), Vol. 5, p. 392.

²⁴J. Haase *et al.*, J. Phys. Chem. **95**, 6996 (1991).

²⁵B. D. Biggs *et al.*, Phys. Rev. Lett. **65**, 2700 (1990).

²⁶M. H. Levitt, Prog. Nucl. Magn. Reson. Spectrosc. **18**, 61 (1986).

²⁷W. W. Warren, Jr., *et al.*, Phys. Rev. B **32**, 7614 (1985).

²⁸M. Rubinstein *et al.*, J. Mater. Res. **1**, 243 (1986).

²⁹G. H. Stauss *et al.*, Phys. Rev. B **35**, 2700 (1987).

³⁰C. Lee *et al.*, Phys. Rev. B **37**, 9053 (1988).

³¹F. Hippert *et al.*, Phys. Rev. Lett. **69**, 2086 (1992).

³²A. Shastri *et al.*, J. Non-Cryst. Solids **153&154**, 347 (1993).

³³D. E. O'Reilly, J. Chem. Phys. **32**, 1007 (1960).

³⁴W. H. Jones *et al.*, Phys. Rev. **132**, 1898 (1963); C. H. Stauss, J. Chem. Phys. **44**, 2719 (1964); J. F. Baugher *et al.*, *ibid.* **50**, 4914 (1969).

³⁵C. P. Slichter, *Principles of Magnetic Resonance* (Springer-Verlag, Berlin, 1990).

³⁶J. Winter, *Magnetic Resonance in Metals* (Clarendon, Oxford, 1971).

³⁷E. R. Andrew and D. P. Tunstall, Proc. Phys. Soc. London **78**, 1 (1961).

³⁸A. Narath, Phys. Rev. **162**, 320 (1967).

³⁹See the footnote on p. 155 of Ref. 35. The details of the derivation can be obtained upon request.

⁴⁰A. Abragam, *The Principles of Nuclear Magnetism* (Clarendon, Oxford, 1961).

⁴¹See, for example, M. Villa and J. Bjorkstam, Solid State Ionics **9–10**, 1421 (1983); S. H. Chung *et al.*, Phys. Rev. B **41**, 6154 (1990); S. R. Elliot and A. P. Owens, *ibid.* **44**, 47 (1991); M. Trunel *et al.*, J. Non-Cryst. Solids **139**, 257 (1992).

⁴²This efficient relaxation mechanism is also present in *i*-Al-Cu-Fe, *i*-Al-Pd-Re, and the approximant phases, whereas the spin-lattice relaxation in Al₂Ru crystal is extremely inefficient [E. Hill *et al.*, (unpublished)].